Deliverable 2.1: Assessment of capabilities of available tools

Aalborg University

This project has received funding from the European Union's Seventh Programme for research, technological development and demonstration under grant agreement No 608597

D2.1: Assessment of capabilities of available tools

Project: DTOcean - Optimal Design Tools for Ocean Energy Arrays

Code: DTO_WP2_AAU_D2.1

	Name	Date
Prepared	Work Package 2 Amélie Têtu (AAU), Jens Peter Kofoed (AAU) Susan Tully (UEDIN) Thomas Roc (IT Power)	14/03/2014
Checked	Work Package 9	20/03/2014
Approved	Project Coordinator	26/03/2014

The research leading to these results has received funding from the European Community's Seventh Framework Programme under grant agreement No. 608597 (DTOcean).

Abstract

In order to make an informed decision on which tools to use in Work Package 2 for hydrodynamic analysis of array layouts of ocean energy converters, an assessment of capabilities of available tools has been carried out and is presented in this report both for wave energy converter arrays and tidal energy converter arrays. This includes their abilities (benefits and drawbacks) with regard to modelling of the individual devices, their interactions within the array and the wave and current (as applicable) transformations through the array area.

Table of Contents

GENERAL INTRODUCTION

Successful industrialisation of ocean energy converters requires deployment of devices in arrays in order to reduce the costs for installation, mooring, cabling, maintenance, etc. The objective of the DTOcean project is to deliver a comprehensive software suite for the development and deployment of such arrays. The specific tools to be developed within Work Package 2 concerns the hydrodynamic analysis of array layouts of ocean energy converters.

This report provides a critical analysis and review of the available tools for hydrodynamic modelling of arrays of ocean energy converters in order to make an informed decision on which tool(s) would be most suitable to underpin the DTOcean software suite for the ranges of application set out in the scope within Work Package 1. Because the physical principle behind wave and tidal energy converters is different, the document has been divided into two parts. The first part describes the numerical tools for modelling arrays of wave energy converters while the second part is dedicated to modelling of tidal energy converters placed in arrays.

PART I: WAVE

1 Introduction

Many different numerical tools have been developed over the last four decades to study the interactions between wave energy converters (WECs) deployed in an array and the impact of the array on the environment. Numerical modelling techniques based on the potential flow equations have been the first techniques developed for modelling arrays of WECs and are still today the most popular tools. Depth integrated and spectral wave propagation models appeared more recently, motivated by the need to gain information on the environmental impact of WEC arrays.

This document reviews the different techniques for numerical modelling of WEC array in order to develop suitable tools for hydrodynamic analysis of array layouts within the DTOcean project. The tools to be developed intend to have the ability to model the individual devices, their interactions with other devices within the array and the wave transformations through the array area.

The fundamental equations and hypothesis behind the reviewed models within the wave section of this document enable to assort them into four categories: potential flow models, depth integrated propagation models, spectral wave models and computational fluid dynamic models. This categorisation helps to compare the models by analysing their benefits and drawbacks. The fundamental behind the modelling techniques are briefly outlined together with the benefits and drawbacks of each technique. A comparative table of the different techniques concludes the wave section within this document.

2 Potential flow models

Potential flow models treat the external flow around wave energy converters for inviscid, incompressive and irrotational flow fields[1]. Since the flow is considered irrotational, a velocity potential function (ϕ) can be defined and the velocity of the fluid (V) can be derived everywhere in the fluid domain, as shown below in equation 1:

$$V = \nabla\phi. \tag{1}$$

From conservation of mass for an incompressible flow, we get the Laplace's equation:

$$\nabla^2\phi = 0 \tag{2}$$

which should be satisfied everywhere in the fluid domain. To obtain the mathematical formulation of the problem, the proper boundary conditions are specified.

[1] An inviscid, incompressive and irrotational flow is an ideal flow assumed to have no viscuosity, constant density and where the fluid particles do not spin as they move.

In order to simplify the problem, the partly or completely submerged bodies are assumed to oscillate with small amplitude about a fixed mean position. Assuming a ratio of wave height to wavelength much smaller than 1, the problem can be linearized. This linearized problem can be solved semi-analytically or numerically using boundary element methods. The following sections describe the different techniques developed to solve the potential flow problem applied to modelling of arrays of wave energy converters.

2.1 Semi-analytical techniques

A considerable amount of work on modelling arrays of wave energy converters have been carried out using semi-analytical representations of a potential flow solution. These representations involve analytical expressions that approximate or converge to an exact solution of the potential flow in the limit of an infinite series. The "Point absorber method", the "Plane wave approximation method", the "Multiple scattering method" and the "Direct matrix method" are the four classes of semi-analytical techniques and they are detailed further in the following sections.

2.1.1 Point absorber method

As its name indicates, the point absorber method ([1],[2] and [3]) is applicable only to heaving point absorbers. The devices are also assumed to be much smaller than the wavelength of the incoming waves, and are all identical bodies and optimally controlled. The body is then considered as a weak scatterer, i.e. the scattered waves are neglected when calculating hydrodynamic interactions. For optimal device motions, the amplitude of the radiated wave is much larger than the scattered one, leading to a consistent approximation for the maximum power absorbed [4]. However, for non-optimal conditions, the amplitude of the radiated and scattered waves are equally important, which can lead to inconsistencies in the approximation of the absorbed power.

2.1.1.1 Benefits

- Calculation of added mass and damping coefficients.
- Calculation of the power absorption as the inverse of a square matrix of order of the number of absorbers in the array.
- Computational efficient for small to medium sized arrays.

2.1.1.2 Drawbacks

- Applicable only for heaving point absorber devices.
- Diffraction from the array not accounted for.
- Inconsistencies in the approximation of the absorbed power for non-optimal conditions.

2.1.2 Plane wave approximation method

The assumption behind the plane wave method is that the spacing between axisymmetric absorbers is large compared to the wavelength of the incoming waves so that, locally and sufficiently far from the structure, the scattered or radiated disturbances are approximated by planes waves[2] ([4]-[7]).

[2] A plane wave is a constant frequency wave whose wavefronts are infinite parallel planes of constant amplitude perpendicular to the direction of propagation.

2.1.2.1 Benefits

- Computational efficient for small to medium sized arrays.
- Diffraction of all waves by each element in the array accounted for.
- Calculation of added mass and damping coefficients and hydrodynamic forces on body surfaces.

2.1.2.2 Drawbacks

- Accuracy reduced in the low frequency range.
- Applicable for heaving point absorber devices.

2.1.3 Multiple scattering method

In principle, the multiple scattering method ([8],[9],[10] and [11]) is a semi-analytical method for calculating, with few assumptions, the excitation forces and associated hydrodynamic parameters of an array of absorbers. The concept is to describe the hydrodynamic interactions as a succession of distinct scattering events. The total wave field around each absorber within an array can be represented by an infinite superposition of the incident wave potential and various orders of propagating and evanescent modes that are scattered and radiated by the array elements. In practice, the infinite summation over horizontal angular and vertical modes and over successive orders of interaction is truncated to finite numbers.

2.1.3.1 Benefits

- Computational efficient for small to medium sized arrays.
- Calculation of added mass and damping coefficients and hydrodynamic forces on body surfaces.
- Possibility to visualize the free surface elevation in the vicinity of the array.

2.1.3.2 Drawbacks

- Mostly applicable for heaving point absorber devices, but can be adapted to other simple geometries.

2.1.4 Direct matrix method

The direct matrix method ([12],[13]) addresses the same problem as the multiple scattering method by simultaneously solving for the amplitudes of all scattered waves, also referred to as modes. In theory, this is an exact method, but in practice, as for the multiple scattering method, the accuracy of the direct matrix method depends on the number of modes taken into account when solving the problem. The solution of the hydrodynamic problem is resumed by the inversion of a square matrix.

2.1.4.1 Benefits

- Computational efficient for small to medium sized arrays.
- Calculation of added mass and damping coefficients and hydrodynamic forces on body surfaces.
- Possibility to visualize the free surface elevation in the vicinity of the array.

2.1.4.2 Drawbacks

- Mostly applicable for heaving point absorber devices, but can be adapted to other simple geometries.

2.1.5 Conclusion

The semi-analytical methods can be a great tool for optimisation routines as they are computationally efficient, but are mostly restricted to simple geometries, predominantly point absorbers. Furthermore, the algorithms for the above mentioned techniques are freely available in the form of research code detailed in articles.

2.2 Boundary element methods (BEM) based on linear potential flow theory:

The differential linear potential flow equations can be discretized and solved numerically by applying the appropriate mathematical function usually in the frequency domain. In this method, the continuous flow field is described in terms of discrete (rather than continuous) values at prescribed locations. The boundary of the flow field is broken into discrete segments and appropriate singularities such as sources and sinks are distributed on these boundary elements. By this technique the differential equations are replaced by a set of algebraic equations that can be solved on a computer. Several BEM commercial tools exist[3] and have been used to model arrays of WECs ([14]-[21]). Recently an open source BEM code called Nemoh [26] has been released by École Centrale de Nantes.

This method is the most popular method used in oil and gas industry, and the experience has shown the method is very reliable in predicting the hydrodynamic performance of the offshore platforms. In wave energy development, the BEM method has been widely used and is probably the most widely used method for studying the hydrodynamic performance of wave energy converters, especially for single device wave energy converters.

2.2.1.1 Benefits

- Calculation of added mass and damping coefficients and hydrodynamic forces on body surfaces for any arbitrary body.
- Possibility to visualize the free surface elevation in the vicinity of the array.
- Can explicitly account for coupled hydrodynamic forces between devices in an array.

2.2.1.2 Drawbacks

- Applies only to small amplitude of motion and wave steepness.
- Applicable only for constant water depth.

2.3 Time-domain formulation

The time-domain formulation is also based on the linear potential flow formulation. Taking the inverse Fourier transform of the frequency-domain equations of motion of an array of N freely floating rigid body WECs yields to equation 3 ([27],[28]):

[3] Commercial tools available: WAMIT [22], ANSYS Aqwa [23], Aquaplus [24], WaveFarmer [25]

$$\mathbf{M}+\mathbf{A}\ \infty\ \ \mathbf{x}(t)+\int_0^t \mathbf{b}\ t-\tau\ \mathbf{x}(\tau)d\tau+\mathbf{K}\mathbf{x}\ t\ =\mathbf{f}(t) \quad (3)$$

where:

- $\mathbf{A}\ \infty$ is the added mass at infinite frequency
- $\mathbf{x}(t)$, the body motions
- $\mathbf{f}\ t$, the wave excitation forces
- **M,** a matrix describing the global mass
- **K,** the matrix of hydrostatic and gravitational restoring coefficients
- $\mathbf{b}\ t$ is the radiation impulse response function and can be obtained from:

$$\mathbf{b}\ t\ =\frac{2}{\pi}\int_0^t \mathbf{B}\ \omega\ \ \cos\omega t\, d\omega \quad (4)$$

The system of equations is discretised using a BEM model.

The potential flow problem can also be solved directly in the time domain. TiMIT [29] is an example of commercially available numerical code solving for the time dependent Green function. This model has mainly been applied to single devices ([30],[31]) but in principle, the method can be applied to arrays as well.

WaveFarmer [25] features also an optional time-domain model to determine array interactions, but it unclear which of the above mentioned time-domain technique is used as the information is not publicly available.

2.3.1.1 Benefits

- Possibility of gaining information on the steady force and moment on the structure.
- Possibility to model transient phenomena and obtaining the impulse-response functions.
- Possibility of including non-linear forces like non-linear viscous damping, mooring and power take-off forces.
- Can explicitly account for coupled hydrodynamic forces between devices in an array.

2.3.1.2 Drawbacks

- Applies only to small amplitude of motion and wave steepness.
- Applicable only for constant water depth.

2.4 Nonlinear potential flow models

Non-linear potential flow models ([32],[33], and [34]) are implemented using a boundary element method in the time-domain. The closed domain in physical space, illustrated in Figure 1: Definition of the computational domain for nonlinear potential flow models (taken from [31]). and often referred to as numerical wave tank, is defined by a set of boundary conditions, as below:

- Γ_b: the bed is impermeable: $\frac{\partial\phi}{\partial n}$ on Γ_b.
- Γ_l, Γ_r: usually a wave generation condition is imposed on the input boundary while a radiation condition on the outflow boundary is imposed: $\frac{\partial\phi}{\partial n}=\frac{\partial\phi}{\partial n}_{known}$ on Γ_l, Γ_r.

- Γ_s: The movement of the free surface must satisfy the kinematic and dynamic free surface boundary conditions ensuring first that the water surface is streamlined and second that the pressure on the water surface remains constant.

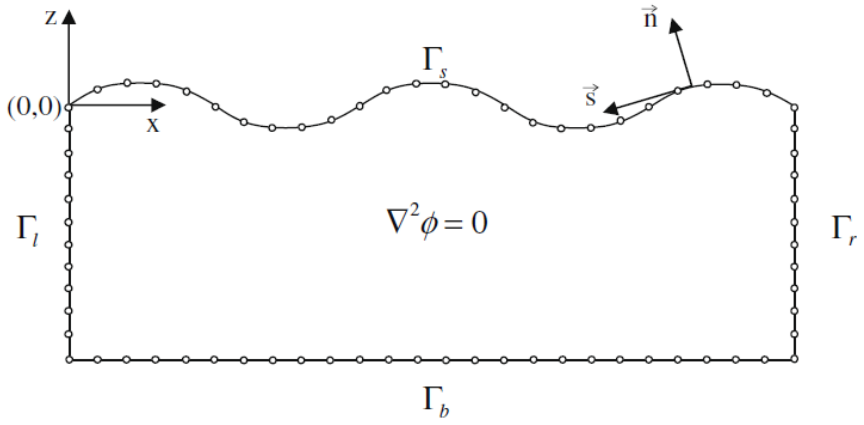

Figure 1: Definition of the computational domain for nonlinear potential flow models (taken from [31]).

The nonlinear potential flow model has not been applied to arrays of wave energy converter yet because of its high computational demand.

2.4.1.1 Benefits

- No requirement on periodicity of the problem, that is an arbitrary definition of body geometries
- Full non-linearity of the problem preserved.
- Definition of a non-uniform bathymetry.
- Can explicitly account for coupled hydrodynamic forces between devices in an array.

2.4.1.2 Drawbacks

- Highly computationally demanding and have not been applied to arrays.

3 Depth integrated wave propagation models

Depth integrated wave propagation models are usually used for modelling nearshore hydrodynamic behaviour and are defined in the time domain.

3.1 Nonlinear Boussinesq models

The nonlinear Boussinesq models are based on the Boussinesq approximation that eliminates the vertical coordinate from the flow equations, while retaining some of the influence of the vertical structure of the flow. The approximation can be applied for waves where the wavelength is large compared with the water depth. Applying the Boussinesq approximation to the flow equations gives a set of nonlinear partial differential equations known as the Boussinesq equations valid for a maximum depth (h) to deep-water wave length (L_o) ratio of $h/L_o \leq 0.22$. This limit was pushed to $h/L_o \leq 0.5$ by Madsen *et al.* [35] who introduced the so-called enhanced Boussinesq equations. The introduced formulation of the Boussinesq equation calculates the free surface elevation based on the flux density leading to better stability. They can be written as

$$\frac{\partial \eta}{\partial t} + \frac{\partial q}{\partial x} = 0$$
$$\frac{\partial q}{\partial t} - Bh^2 \frac{\partial^2 q}{\partial x^2}\frac{\partial q}{\partial t} - \frac{1}{3}h\frac{\partial h}{\partial x}\frac{\partial q}{\partial x}\frac{\partial q}{\partial t} + \frac{\partial\ uq}{\partial x} + gH\frac{\partial \eta}{\partial x} - \beta g h^3 \frac{\partial^3 \eta}{\partial x^3} - 2\beta g h^2 \frac{\partial h}{\partial x}\frac{\partial^2 \eta}{\partial x^2} = 0 \quad (5)$$

where:

- $\eta(x,t)$ is the surface elevation
- $h(x,t)$, the depth at still water
- $H\ x,t\ = \eta\ x,t\ + h(x)$, the total depth
- g, the gravitational acceleration
- B and β, numerical parameters obtained by optimizing the dispersion properties of the linearized model with respect to the Airy wave theory [36]
- $q(x,t)$, the discharge $q = Hu$, where u denotes the depth averaged speed.

The Boussinesq wave editor (MIKE 21 BW [37]), part of the MIKE 21 suite of software developed by the Danish Hydraulic Institute Water and Environment, is a software based on the enhanced Boussinesq equations. This model was applied to the case of arrays of WECs as described in [38] and [39].

3.1.1 Benefits

- Calculation of diffraction, refraction, shoaling, wave breaking, non-linear wave-wave interactions and bottom dissipation processes.
- Non-linearity of the problem preserved.
- Can handle partial reflection and wave transmission from partially reflecting porous structures, directional wave spreading and internal wave generation.
- Includes frequency dispersion

3.1.2 Drawbacks

- Computationally demanding

3.2 Linear Mild-slope models

Mild-slope models are based on the mild-slope equation describing the propagation and transformation of water waves over varying bathymetry and with lateral boundaries. This is a linear model that calculates the velocity potential and surface elevations throughout the numerical domain with low computational cost. For a free surface elevation $\eta(x,y,t)$ and a mean water depth $h(x,y)$ the mild-slope equation is:

$$\nabla.\ c_p c_g \nabla\eta\ + k^2 c_p c_g \eta = 0 \quad (6)$$

where:

- c_p and c_g are the phase velocity and the group velocity respectively
- k, is the wavenumber of the wave

MILDWave [40] is a numerical model developed at Ghent University based on the mild-slope equations of Radder and Dingemans [41].

REF/DIF [42] is another linear mild-slope wave propagation model developed at the University of Delaware.

The OLUCA_SP model [43] that solves the parabolic version of the mild-slope equations can also be used to study arrays of WECs.

3.2.1 Benefits

- Calculation of refraction, shoaling, diffraction, wave breaking, bottom dissipation processes.
- High stability performance.
- Relatively low computational cost.

3.2.2 Drawbacks

- Not capable of modelling nonlinear wave dynamics

4 Spectral wave models

The spectral wave model ([44], [45], and [46]) defines another category of numerical model predicting the average properties of the wave field (surface wave frequency and directional spectrum) propagating in deep water. This type of model was later adapted for wave field propagating in shallow water taking into account varying water depth and background currents. This type of model is based on the conservation of wave action, which is the spectral density divided by the intrinsic frequency, and is capable of simulating wave propagation processes like diffraction and reflection, and wave generation processes, but also dissipation processes that occur in shallow water like bottom friction, wave breaking and white capping dissipation together with wave-wave interaction.

The representation of a WEC array has been carried out in two different ways: the supra-grid method where the WEC array is defined over several grid points and the sub-grid method where each WEC in the array is represented at a single computational grid point. These two different approaches are described below.

4.1 Supra-grid models

Three studies have used supra-grid spectral wave model for modelling arrays of WEC ([47], [48], and [49]).

Millar *et al.* [47] defined a 4 km obstacle to describe an array of WECs, with a constant transmission coefficient through the whole spectrum, and they estimated the effect the altered waves had on the coastline. This method does not account for the frequency dependent energy absorption. The frequency dependency of the energy absorption was introduced in 2012 [48] through a frequency dependent transmission coefficient.

The SWAN wave propagation model [50], developed at Delft University of Technology, is an open source software available for supra-grid spectral wave modelling. This model propagates wave energy through a grid, calculating the evolution of the spectrum by solving the action balance

equation for action density $N(\sigma,\theta)$, the energy density divided by the angular frequency relative to any currents present, σ, where θ is the wave direction. The action balance equation is given by:

$$\frac{\partial}{\partial t}N\ \sigma,\theta\ +\frac{\partial}{\partial x}c_x N\ \sigma,\theta\ +\frac{\partial}{\partial y}c_y N\ \sigma,\theta\ +\frac{\partial}{\partial \sigma}c_\sigma N\ \sigma,\theta\ +\frac{\partial}{\partial \theta}c_\theta N\ \sigma,\theta\ =\frac{S(\sigma,\theta)}{\sigma} \quad (7)$$

where:

- c_x and c_y are the velocity components of $N(\sigma,\theta)$
- c_σ and c_θ, the propagation velocities in the σ- and θ- space
- $S\ \sigma,\theta\ $, the source term representing the generation, redistribution and dissipation of energy in the spectrum.

Sandia National Laboratories has developed a modified version of SWAN called SNL-SWAN [49]. SNL-SWAN maintains all of the capabilities of SWAN, while adding new transmission coefficient models for obstacles. SNL-SWAN, like SWAN, is open source software. While SWAN models obstacles using constant transmission and reflection coefficients, SNL-SWAN has the capability to apply a transmission coefficient which varies with sea state.

4.1.1 Benefits

- Calculation of depth and current induced refraction, shoaling, wind forcing, white-capping and bottom friction dissipation, dissipation through bathymetric breaking, and nonlinear quadruplet and triad wave-wave interactions.
- The diffraction can be approximated [44].

4.1.2 Drawbacks

- Does not account for the radiation of energy by the WECs.

4.2 Sub-grid models

Sub-grid spectral wave models treat each WEC of an array, situated at a computational grid point, as a source and sink of wave energy, and this as a function of frequency ([51],[52]). This way, the energy absorption and radiation of each individual WEC is taken into account in the overall calculation.

The TOMAWAC wave propagation model [53], developed by Électricité de France, is an open source software available for sub-grid spectral wave modelling. It uses a finite-element type method to solve the simplified equation for the spectro-angular density of wave action. This is carried out for steady-state conditions, i.e. with a fixed depth of water throughout the simulation.

WaveFarmer [25] includes also a modified version of the TOMAWAC wave propagation model.

4.2.1 Benefits

- Calculation of depth and current induced refraction, shoaling, wind forcing, white-capping and bottom friction dissipation, dissipation through bathymetric breaking, and nonlinear quadruplet and triad wave-wave interactions.
- The diffraction can be approximated [44].
- Frequency dependent energy absorption.
- Accounts for the radiation of energy by WECs.

4.2.2 Drawbacks

- Phase-dependent processes, like near field effects around each individual WEC are not explicitly modelled.

5 Computational fluid dynamics models

Computational fluid dynamics (CFD) models are based on the Navier-Stokes equations derived from mass, energy, momentum and angular momentum conservation, taking into account viscous effects and turbulence. When applied to wave energy converters, the fluid flow fluctuations in time and space due to turbulence are averaged and these mean values are considered to be steady in the time interval of the computation. This leads to solving the transient Reynolds-average Navier-Stokes equations, which are time-averaged equations of motion for fluid flow, where the numerical domain is discretised with finite difference, finite element or finite volume scheme, the latter being the most popular scheme because of its versatility.

5.1 Benefits

- Ideal for simulating extreme wave loads.
- Retains the full non-linearity of the hydrodynamics.
- Possibility of describing currents.
- Can explicitly account for coupled hydrodynamic forces between devices in an array.

5.2 Drawbacks

- Computationally demanding.

.

	Potential flow models				Depth integrated wave propagation models		Spectral wave models		CFD
	Semi analytical models	Linear freq. domain BEM	Time-domain BEM	Nonlinear BEM	Boussinesq	Mild-slope	Supra-grid	Sub-grid	
Fundamental									
Definition of hydrodynamics	Implicit body surfaces, explicit coefficients				Explicit absorption layers		Explicit absorption layer	Explicit source strength	Implicit fluid flow
Hydrodynamic coupling	Explicitly capable	Explicitly capable	Explicitly capable	Explicitly capable	Approximation through frequency dependent absorption		Approximation though frequency dependent absorption		Explicitly capable
Nonlinear wave dynamics	Not capable			Implicitly capable	Implicity capable	Not capable	Implicitly capable for phase-averaged dynamics		Implicitly capable
Nonlinear dynamics	Not capable		Implicit solver		Explicit absorption layers		Explicit absorption layer	Explicit source strength	Implicit solver
Vortex shedding	Explicit inclusion by linearisation		Explicit inclusion		Explicit inclusion		Explicit inclusion		Implicit inclusion
WEC radiation	Implicitly capable				Explicitly capable		Not capable	Explicitly capable	Implicitly capable
Diffraction	Implicitly capable				Explicitly capable		Approximated by phase-decoupled refraction-diffraction		Implicitly capable
Variable bathymetry and marine currents	Not capable				Implicity capable within certain conditions		Implicitly capable		Implicitly capable
Computational									
Primary dependent	Complexity of function	# of panels	# of panels and complexity of equations	# of panels	# of cells		# of cells		# of cells
Secondary dependent	# of frequencies and directions		# of time-steps		# of time-steps		# of frequencies and directions		# of time-steps
Determinate of array size	Quadratic increase with number of WECs				Linear increase with spatial area		Linear increase with spatial area		Linear inc. with spatial volume
Solver	Simple and stable		Simple and poss. unstable	Complex and stable	Simple and poss. unstable	Simple and stable	Simple and stable		Complex and poss. unstable
Usability									
Required skills	High	Low	Medium	High	Medium	Low	Low	Medium	High
Software available	Research code only	Commercial and open-source code	Commercial code	Research code only	Commercial code available, WEC model required		Open-source code available, WEC model required		Commercial and open-source code
Suitability	scale 0-3 -> 0: not suitable, 3:higly suitable								
Localised effects	0-3	2	2	2	1	1	0	0	3
Dynamic control	0	0	3	3	0	0	0	0	1
AEP (small WEC array)	2	2	1	1	2	2	1	2	1
AEP (large WEC array)	2	1	1	1	2	2	1	2	1
Environmental impact	0	0	0	0	2	2	3	3	1

PART II: TIDAL

1 Introduction

Developing a marine array project is an iterative process aiming to optimise, in parallel, several distinct features such as the cost/benefit ratio, the return on investment (ROI), the project life cycle and the socio-environmental impacts. In order to obtain relevant outcomes this process needs to account for all the technical components involved from the design to the operation phase. As well as revolve around accurate modelling of the physical processes driving the system and their sensitivities to the technical component variations. In the case of tidal array projects this leads to reliable hydrodynamic modelling, especially wake interactions, imposing itself as a prerequisite.

Being too complex to be resolved analytically, numerical models are required to simulate such processes. Additionally, because of the wide range of technical components to be accounted for as well as their inter-dependencies, trade-offs between computational cost and numerical accuracy have to be made in order to reach an acceptable solution within the required timescale. [54]. Computational cost can be reduced by the use of coarse or adaptive grids or by utilising numerical optimisation techniques such as parallel computation. Or by using simplified hydrodynamic models or semi-empirical approaches.. However, by simplifying the physical processes controlling the application, you can introduce the risk of generating incorrectly optimised solutions.

This document gathers and describes the most up-to-date methods for tidal array modelling. It aims to aid and facilitate the decision-making process regarding the choice of hydrodynamic modelling method which will be used in the DTOcean software suite pre-alpha version. Each method is described by three items: Theory, Benefits and Drawbacks.

2 Parametric models

The simplest and least computationally expensive approaches to tidal array modelling are the parametric modelling approaches. Most physical processes contain far too many degrees of freedom to allow for a useful parametric analysis to be done. By reducing the physical processes down to a set of parameters which can be used to define your model you can gain an understanding of the key parametric relationships within your model and optimise them efficiently. The solution is reached iteratively, constraining and optimisation occurring with respect to the whole matrix of parameters in parallel. Most times parameters are constrained to match empirical evidence or physical

constraints. Such methods provide a good understanding of the basic behaviour being simulated which can then provide the input to more detailed computational fluid dynamics modelling of if required.

2.1 Drag coefficient model

This one dimensional approach [55] is based on the shallow water momentum balance rewritten in terms of non-dimensional transport $U'\ t\ = \frac{a*u(x,t)}{\omega*W\ x\ h(x)}$ and integrated along the channel:

$$I\frac{\partial U'}{\partial t'} = \sin\ t' + \phi_g\ - \alpha[BC_D^* + C_F^*]\ U'\ U' \qquad (8)$$

where:

- a is the parameter related to both tide amplitude and gravity wave propagation (see [56])
- u, along channel velocity
- ω, forcing frequency
- W, channel width
- h, channel water depth
- I, B, geometric factors (see [56])
- t', non-dimensional time ($t' = t * \omega$)
- ϕ_g, phase (see [56])
- α, non-dimensional parameter introduced for conciseness (see [56])
- $\lambda_0 = \alpha B C_D^*$, effective background bottom drag coefficient
- $\lambda_T = \alpha C_F^*$, farm's gross drag coefficient

By applying Bernoulli, mass and momentum conservations within control volumes, one can express the farm's drag coefficient λ_t as a function of the non-dimensional number of rows N_R^*, the fraction of cross-section taken by the turbines ϵ and the wake velocity r_3 also described as "turbine tuning parameter" or "turbine pitch parameter".

In order to combine the models from Garrett and Cummins [57] and [58] , specified values for N_R^*, ϵ and r_3 have been used to calculateλ_t. From this combined model, numerous benchmarks charts for the peak power loss$C_{F_{peak}}^*$, the farm's optimal drag coefficientC_F^{*opt}, the Farm Efficiency Index (FEI) or the economic efficiency of Turbine Efficiency Index (TEI) have been computed and discussed.

2.1.1 Benefits

- Permits a fast and simplified resource assessment.
- Layout spacing and blade-pitch optimisation of tidal turbines are based on both site and device specific features.

2.1.2 Drawbacks

- Based on restrictive assumptions such as:
  - Uniform rectangular channel
  - Turbines arranged on a grid

  - Tidal currents uniform across channel
  - Tidal forcing of single frequency
  - Spacing between rows are large enough to allow for full flow recovery (which causes wake decay).
  - The application of this method is limited to Small Froude number flow and therefore large enough spacing between turbines is required such that: $\frac{r_4 a U_0}{\omega \sqrt{gh}} \ll 1$.
- Model does not account for, nor simulate:
  - Free surface effects such as hydraulic jump in blockage scenarios
  - Flow and/or device-induced turbulences
- Lack of information concerning validation against experimental or in-situ data.

2.2 Semi-empirical wake model

The semi-empirical wake model [59] combines two semi-empirical models, one simulating the wake expansion behind a turbine (i.e. Jensen model) using mass conservation through the rotor plan. The other accounts for the wake interactions using momentum conservation. The Jensen model is a semi-empirical model describing the velocity field in the wake. This model was initially developed for wind turbines and thruster-thruster interaction and based on the momentum balance. The governing equations are:

$$\begin{aligned} &\pi r_0^2 U_{w0} + \pi(r^2 - r_0^2)U_0 = \pi r^2 U_w \\ &r = r_0 + kx \\ &U_{w0} = U_0 \sqrt{1 - C_t} \end{aligned} \tag{9}$$

where:

- r_0 represents the turbine radius
- r, the wake radius
- U_0 inflow velocity
- U_{w0} flow velocity at the device location
- U_w flow velocity in the wake
- k empirical wake decay coefficient.
- x distance along the rotor centre-line
- C_t thrust coefficient

Note that k requires calibration against data as it is closely related to ambient turbulence levels.

The wake interaction model is based on the superimposition of wake velocities. Three main scenarios of wake interactions are identified and designated as “Tandem”, “Interference” and “Overlap”.

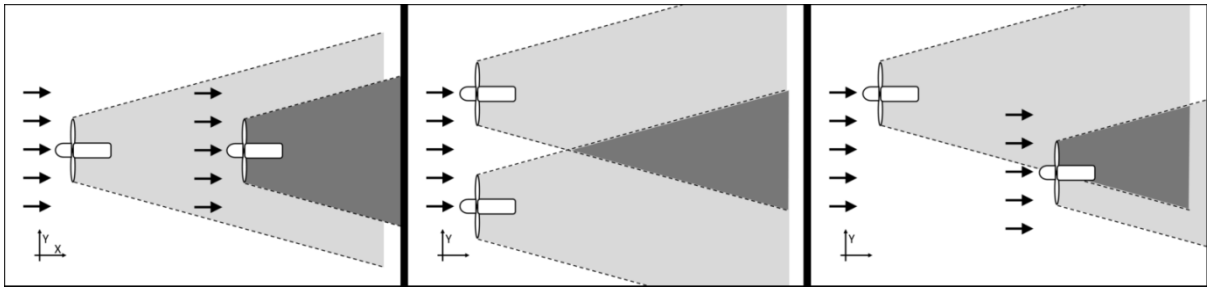

Figure 2: Different scenarios. From left to right, "Tandem", "Interference" and "Overlap". Adapted from figures 5, 6 and 7 in [59]

In “Tandem”, the velocity experienced by the downstream turbine can be easily estimated with the Jensen model. In “Interference”, five different analytical methods are proposed in the reference relationships to estimate the velocities in the different wake regions [59]. As for the “Overlap”, two methods are proposed, both based on geometrical considerations. The first method uses the mass conservation through the rotor plane, whereas the second uses momentum conservation

2.2.1 Benefits

- Permits a fast and coarse simulation of the velocity field and wake interactions within tidal turbine arrays.
- Validation against CFD simulations of simplistic scenarios shows 90% accuracy for velocity prediction.

2.2.2 Drawbacks

- The base assumptions are restrictive:
    - Complex flow patterns of the near wake are neglected (i.e. 0 to 5 diameter downstream of the device)
    - Turbine simulation using actuator discs; far wake is not influenced by detailed turbine design
    - Surface and bottom boundary effects are neglected, thus wakes are assumed axis-symmetric
    - Steady state (flow variations are slow compared to the blade rotational motion)
    - No upstream interaction (row spacing larger than 5 diameters)
    - Spatially uniform flow velocity fields
- Method does not account for turbine induced turbulence.
- The 10% error in velocity prediction listed in the benefits above leads to a 33% error in power prediction as the velocity is cubed.

2.3 Blockage and efficiency model

The main assumption of this model [60] is that for a sufficiently large array, the flow around each turbine should be considered three-dimensional and has a characteristic length scale equivalent to the turbine-diameter d whereas the flow around the entire array can be considered as two-

dimensional and has a characteristic length scale equivalent to the array width. Consequently all device-scale flow events, viscid and inviscid, occur much faster than the horizontal expansion of the flow around the entire array. As a result, the flow system can be modelled with a combination of two quasi-inviscid problems of different scales.

Thereafter, three different blockage parameters are defined, B_A the array blockage, B_L the local blockage and B_G the global blockage:

$$B_A = \frac{1+\frac{s}{d}}{\frac{w}{nd}}$$
$$B_L = \frac{\pi}{4\frac{h}{d}\ 1+\frac{s}{d}} \quad (10)$$
$$B_G = B_A B_L$$

where:

- s represents the intra-turbine spacing (m)
- w channel width (m)
- n number of turbines
- h water depth (m).

Similarly, three induction factors $a_{L,A,G}$, three thrust coefficients $C_{T_{L,A,G}}$ and three power coefficients $C_{P_{L,A,G}}$ are defined:

$$a_L = 1-\frac{U_D}{U_A}\ ; C_{T_L} = \frac{Thrust_D}{\frac{1}{2}\rho U_A^2 \frac{\pi d^2}{4}}; C_{P_L} = \frac{Power_D}{\frac{1}{2}\rho U_A^3 \frac{\pi d^2}{4}}$$
$$a_A = 1-\frac{U_A}{U_C}\ ; C_{T_A} = (1-a_A)^2 B_L C_{T_L}; C_{P_A} = (1-a_A)^3 B_L C_{P_L} \quad (11)$$
$$a_G = 1-\frac{U_D}{U_C};\ C_{T_G} = \ 1-a_A\ ^2 C_{T_L};\ C_{P_G} = \ 1-a_A\ ^3 C_{P_L}$$

where:

- U_D represents the streamwise velocity at the device $(m.s^{-1})$
- U_A represents the streamwise velocity at the fence $(m.s^{-1})$
- U_C represents the streamwise velocity in the far wake region $(m.s^{-1})$.

In order to close this equation system, the conversation of mass, momentum and energy is then considered in each local flow passage and thereafter at the array scale. Ultimately, the entire set of thrust and power coefficients is uniquely determined and numerical solved for a given value of a_L.

2.3.1 Benefits

- The efficiency of one-row long arrays and tidal fences can be easily explored.
- The model permits and exhibits that efficiency optimisation can be performed using local and global blockage effects.

2.3.2 Drawbacks

- The base assumptions are restrictive:
  - Mass flux through the channel is constant which is not true if induced drag becomes significant compared to the drag along the entire channel
  - Effects of changes in water depth are neglected
  - Channel is considered rectangular and uniform with constant and uniform inflow
  - Intra-turbine spacing is constant along the array
  - Only one-row array is covered. Method assumes full wake recovery within inner turbine scale model and so cannot be used for multiple row layouts.
  - Flow is assumed incompressible and inviscid everywhere except for in the far wake region
- Method does not give insight on turbine induced influences.
- There is lack of information concerning validation against experimental or in-situ data.

2.4 Combination of blockage and wake model

This commercial model, TidalFarmer [61], is a combination of a "blockage model", effecting rotor performance, loading and surrounding flow, and a "near wake model" initialising a "far wake mixing model". The "blockage model" is based on a 3 dimensional potential flow model in which the flow velocity components (u, v, w) are expressed as follows:

$$u, v, w = U, V, W + \frac{m}{4\pi}\frac{r}{r^2} \quad (12)$$

where:

- U, V, W are the average components of the flow velocity as defined in the Reynolds decomposition $(m.s^{-1})$
- m source of strength to be determined (unknown units)
- r is not defined in the reference.

The "near wake model" derived from semi-empirical relationships developed in the wind turbine field ([62], [63], [64]) and extended to stream turbines thanks to the PerAWaT experiment program. In essence, the aim of the "near wake model" is to identify when and where the flow satisfies the criteria of self-preservation and therefore where and when the "far wake model" becomes valid. This is a proprietary model and the details have not been made publicly available. It may be that co-operating with PerAWaT would yield more information.

The "far wake model" is based on the free-shear flow equations:

$$u\frac{\partial u}{\partial x}+v\frac{\partial v}{\partial y}=-u\frac{\partial}{\partial y}\left(\nu_t\frac{\partial u}{\partial y}\right)+\cdots+v\frac{\partial}{\partial z}\left(\nu_t\frac{\partial u}{\partial z}\right)$$
$$\nu_t=F\kappa B\left(U_i-U_c\right)+\varepsilon \qquad (13)$$
$$\frac{\partial u}{\partial x}+\frac{\partial v}{\partial y}=0$$

where:

- ν_t represents the Reynolds shear stress
- F, filter function
- κ, Von Karman constant
- B, wake width
- U_i-U_c , velocity difference across the shear layer
- ε, ambient mixing

2.4.1 Benefits

- Extended calibration and validation has been conducted on this model, which consequently shows a high level of accuracy.

2.4.2 Drawbacks

- TidalFarmer is a commercial model and publicly available information on its workings is limited. This makes an impartial assessment regarding the method's applicability, limitations and overall relevancy difficult.

3 Depth-averaged Navier Stokes models

The approaches in this section are based on the two-dimensional, depth-averaged Navier Stokes equations, commonly referred to as the shallow water equations. The basic assumption of the shallow water equations is that the vertical scale of your flow is much smaller than the horizontal scale so that you can average over the depth to remove the need for three-dimensional analysis.

3.1 Momentum sink model

This model [65] is a modification of Cardiff University's open source hydro-environmental model – DIVAST (Depth Averaged Velocity and Solute Transport) [66]. DIVAST was designed for estuarine and coastal modelling and assumes little vertical stratification in the flow. It can simulate two-dimensional unsteady flows with surface elevations and bed topography included. DIVAST solves the shallow-water equations using a finite-difference alternating direction implicit (ADI) approach [67]. Turbines are represented as momentum sinks that apply an external force in the momentum equation. This force has two components – a reaction, F_{Tx}, to the axial thrust of the turbine and a drag force, F_{Dx} , due to the support structure. These forces are per unit area in the x = constant plane.

Calculation of the axial thrust, *T*, requires knowledge of the thrust coefficient C_T (assumed constant) taken from the relevant tip speed ratio (TSR), hub pitch and flow velocities. The DTOcean project has

access to typical values for C_T from CACTUS (Code for Axial and Cross-flow TUrbine Simulation) simulations and scaled turbine measurements carried out by Sandia National Laboratories. CACTUS is an open-source design and analysis tool for hydrokinetic turbines. The thrust is:

$$T = \frac{1}{2} C_T \rho A U_{eff}^2 \tag{14}$$

where:

- C_T = thrust coefficient
- A = swept area of turbine
- U_{eff} = effective flow velocity, parallel to the turbine's rotational axis. U_{eff} is the same as the bulk flow velocity if the turbines are perpendicular to the flow

The total reactive thrust force per unit area, F_T, calculated by dividing the reactive thrust by the area of a cell, is:

$$F_T = \frac{T}{\Delta x \times \Delta y} \tag{15}$$

where:

- $\Delta x, \Delta y$ = the mesh cell dimensions.

The *x* and *y* components of this, F_{Tx} and F_{Ty} respectively, can be calculated as follows:

$$F_{Tx} = F_T \times \sin\theta \times \sin u \tag{16}$$

$$F_{Ty} = -F_T \times \cos\theta \times \cos v \tag{17}$$

where:

- θ = angle of the turbine's rotational axis to the positive *y* direction
- u, v = *x, y* velocity components respectively

Calculation of the structure-induced drag follows a similar route, with C_T replaced with C_D and the area, *A,* referring to the pile cross-sectional area perpendicular to the flow.

Solute transport can also be accounted for upon depth integration of the three-dimensional solute mass balance equation if required. This method assumes incompressible and unsteady turbulent flows with turbulence represented by a depth-integrated eddy-viscosity model – chosen for its superior performance in modelling tidal eddies over a simple mixing length model.

Fallon [68] uses a similar approach, although he only considers freely rotating turbines that are always perpendicular to the flow. Note that in far-field models the grid spacing will frequently be much larger than the diameters of the turbines themselves. This allows for multiple turbines to reside in a single grid cell. This method averages the forces over each grid cell.

3.1.1 Benefits

- Structured grid – external forces calculated per unit area.
- Based on an open source model.
- Computational overhead reduced because the ADI approach does not solve a complete two-dimensional matrix [68].
- Inclusion of surface and seabed effects – wind shear, bottom roughness; as well as Coriolis forces.
- Also models sediment transport and bacteria sediment interaction if required.
- Model allows for representation of turbines that are fully free to rotate as well as those that are fixed.
- Not overly sensitive to mesh size [69].
- Allows for any layout of turbines.
- Allows for the simulation of whole, large, test sites.
- Allows for water surface elevation analysis.

3.1.2 Drawbacks

- Model has been tested against one-dimensional modelling results due to lack of published data.
- Basic momentum sink model – does not account for resolved blade effects.
- Thrust coefficient assumed constant for turbines.
- No turbulent wake effects represented.
- Does not capture bypass flows – likely to over predict far-field impacts as a result.

3.2 Adaptive mesh – depth averaged friction model

Gerris [70] is an adaptive mesh, finite-volume solver for the shallow water equations with a linear free surface approximation [71]. Instead of focusing on Reynolds-averaged flow, this method focusses on the time-dependant dynamical wake structure and associated vorticity distributions. The mesh resolution varies with calculated vorticity such that the higher the turbulence, the more resolved the flow region. This captures a broad spectrum of turbulent length scales from device-specific wake structures to the largest channel width without the need for a computationally expensive fixed mesh. The authors state that this yields a 10% improvement in computation time as compared to a similarly resolved fixed mesh. Flather [72] boundary conditions are used on the inlet and outlet to reduce reflections back into the computational domain.

The turbines themselves are represented by rectangular regions of increased depth averaged friction. Similar to the approach used by [73] and [74], the drag coefficient in each cell represents an average of the total drag due to structure impedance, energy extraction, and free stream drag-free flow. The optimal drag coefficient is calibrated against data for a single, laboratory-scale turbine. The total power removed by the array over a complete tidal cycle is then:

$$P = \int_{turbine\ area} \frac{1}{2} \rho C_d U^2 \ U \ dA \qquad (18)$$

where

- C_d = depth-averaged drag coefficient per unit width
- A = individual turbine cross-sectional area
- U = incident flow velocity

Gerris relies on low-level background bottom friction and numerical dispersion to damp out turbulence indicating that vorticity is slow to dissipate when compared to a sub-grid scale closure method. While this allows for a more turbulent channel, the wake decay distance will be affected leading to errors in the estimated power production for downstream turbines. There is no ambient turbulence model included; the author's rely on turbine induced turbulence. As this is slow to dissipate in their model the channel becomes increasingly turbulent with each tidal pass.

3.2.1 Benefits

- Can model full and multiple tidal cycles easily.
- Drag coefficient (used for energy extraction) calculated using the flow rate directly entering the cell of interest and not a global constant flow rate allowing for better analysis of device layout effects on predicted power output.
- Accounts for shear-induced vorticity around the rectangular turbine representations allowing for more mixing of the flow.
- Adaptive mesh allows for conservative meshing.

3.2.2 Drawbacks

- Power extraction set by a drag coefficient that represents both the structural drag and energy extraction – hard to quantify device design effects.
- No induced wake rotation.
- More computationally expensive than other 2D methods given the required resolution around the turbine, although this is partially mitigated by the adaptive mesh.
- No ambient turbulence modelled.
- Turbulence dissipation reliant on low-level background bottom friction and numerical dispersion which leads to slower decay than could be expected.

3.3 Seabed friction model – modified POLCOMS

Turbines are represented as additional seabed friction source terms in the depth-averaged POLCOMS (Proudman Oceanographic Laboratory Coastal Ocean Modelling System) model ([75], [76]), while the effects of wind stress and atmospheric pressure are neglected. Turbulence closure is provided by the Mellor-Yamada-Galperin [77] level 2.5 scheme – a 2-equation 2nd order model.

The model incorporates tidal turbines by assuming each has a constant power coefficient, C_p, above the cut-in speed and that the flow direction is normal to the span-wise cross section of the array. From this, the power extracted per device, *P,* can be calculated from the magnitude of the instantaneous incident velocity, *U*.

$$P = \frac{1}{2}\rho A_T U^3 \tag{19}$$

where:

- ρ = density of sea water
- A_T = Cross sectional area of energy extraction plane

This is then converted to bed friction terms, p_x and p_y which equate to the power extracted per grid cell:

$$p_x = -nC_p \frac{P}{\rho UAH} cos\,\theta \tag{20}$$

$$p_y = -nC_p \frac{P}{\rho UAH} \sin\theta \tag{21}$$

where:

- θ = direction of current
- n = number of turbines contained within grid cell
- C_p = Coefficient of power, assumed constant
- A = Area of singe grid cell

3.3.1 Benefits

- Low computational cost.
- Can be applied to any farm size and layout
- Useful if considering the regional-scale effects of arrays in oceanographic models when larger grid size is acceptable.
- Turbulence included to 2nd order accuracy.
- Parametric method can be used to adapt other existing oceanographic models.

3.3.2 Drawbacks

- Assumes constant power coefficient above cut-in speed.
- Assumes turbines free to rotate and are always perpendicular to flow direction
- No device-scale wake effects or interactions.
- Predicted power misrepresented by lack of turbulent mixing modelled
- No accounting for bypass flow.

- Makes the assumption that flow is normal to the array in the power calculations despite accounting for the flow direction in the friction terms. This could overestimate power production.

3.4 Turbine drag model

The commercial SMARTtide software suite [78] is built upon the open-source TELEMAC-2D [79] module system for free-surface flow – a finite-element solver for the two-dimensional depth-averaged shallow water equations with free surface flow. TELEMAC relies on unstructured, triangular grids allowing for smooth transition from high resolution areas of interest to coarse-gridded regions. Tidal array schemes are represented within SMARTtide by body force terms added to the shallow water equations. These additional drag terms take the form:

$$F_e = -\frac{power\ curve}{U} \tag{22}$$

$$F_D = -\frac{1}{2}\rho\ U\ ^2 C_D A \tag{23}$$

where:

- F_e, F_D = energy extracted and specific device drag.
- $power\ curve$ = device power curve, model input
- U = norm of depth averaged velocity
- ρ = water density
- C_D = Structural drag coefficient
- A = associated area

Energy removed from the system by tidal devices is based on the norm of the depth-averaged velocity and SMARTtide is capable of modelling both the energy take off of a tidal barrage and open arrays of tidal devices. The SMARTtide model was designed as an industrial tool to estimate the large-scale impacts of turbine arrays on tidal ranges and tidal currents. The model is based on spatially varying time histories of water levels along its offshore boundaries. These water levels are derived from the TPXO dataset [80] – a highly accurate global model of oceanographic tides.

The software includes two pre-meshed (from Admiralty Chart data) domains of interest given below. Both extend from beyond the northern European continental shelf to the north western coast of Europe:

- Coarse Continental Shelf Model (CCSM) – A coarse grid with resolution ranging from 1km along coastlines and regions of interest to 35km in open water.
- Detailed Continental Shelf Model (DCSM) – A more detailed mesh of the same region, but that ranges from 10km down to 200m in resolution.

Users would be required to input the following data about their tidal scheme: the number of devices per square km, a structural drag coefficient, a device footprint, and a thrust or power curve.

It should be noted that TELEMAC-2D is open source and relevant bathymetric and tidal forcing data are available online. Similar studies have been carried out using TELEMAC-2D alone [81].

3.4.1 Benefits

- Code can be run in parallel. Authors report that on 20 processors the CCSM model (160,000 nodes) above simulated 17 days in 35 minutes of wall clock time. TELEMAC itself has good scaling performance on massively parallel computer architectures [82].
- Fully packaged with a user interface and support.
- Baseline model is well validated against two independent data sets: coastal and offshore tidal gauge measurements, and bottom-pressure data.
- Also validated against the UK Marine Renewable Energy Resource Atlas.

3.4.2 Drawbacks

- Usable on a fee-for-service basis.
- Designed more for whole array site choices rather than internal array layout and spacing.
- Designers note that SMARTtide is not meant to be a tool to replace a detailed numerical investigation of site-specific array behaviour.
- The smallest resolution is 200m.
- Device-specific flow behaviour (wake mixing etc.) not accounted for.

4 Computational fluid dynamics models

The methods given in this section are based on solving the three-dimensional Navier Stokes equations. These models are commonly referred to as computational fluid dynamics (CFD) models. The CFD approach is the most computationally expensive method for modelling tidal arrays given the requirement for both three-dimensional modelling and higher mesh resolutions. The plus side is that you can include more flow phenomena into your model directly, without the need for empirically derived parameters or approximations. The methods covered here are those that are most suitable to large scale modelling as is required for the DTOcean project. Methods such as actuator line, actuator surface and blade resolved approaches are not covered as their computational requirements do not fit the remit of the DTOcean project.

4.1 Blade element momentum theory model

The Reynolds Averaged Navier-Stokes – Blade Element Momentum Theory (RANS-BEMT) approach ([83], [84]) is a popular three-dimensional method for representing turbines in small to medium scale simulations ([83], [84], [85]). The requirement that the mesh must resolve the swept area of each turbine limits the use of this approach in large-scale simulations. This relatively high mesh resolution is required in order to allow for changes in lift and drag along the blade length (swept area radius).

Turnock *et al.* [83] use the BEMT code Cwind [86], an in-house code at Southampton University however similar open-source codes exist ([87], [88]). Originally written for predicting wind turbine

stall behaviour Cwind has been modified to account for the differences when modelling tidal turbines [89].

A three-dimensional Reynolds-averaged domain surrounds, and is coupled to, a cylindrical domain where an individual turbine is represented through the momentum source term *f*. The cylinder has a diameter equal to that of the turbine swept area and is usually around 10-30% of the diameter in thickness. The volume of the cylinder is divided into radially increasing annuli. Within each of these annuli, BEMT is used to calculate local thrust and power coefficients corresponding to the relevant blade cross-section at that radius, the incident flow velocity from the larger RANS simulation and the corresponding angle of attack for a given TSR. These coefficients are then used to calculate the thrust, *T,* and torque, *Q,* within each annuli as follows:

$$T = \frac{1}{2}\rho U_0^2 A \delta C_T \tag{24}$$

$$Q = \frac{1}{2}\rho U_0^3 A \delta C_P \tag{25}$$

where:

- T = axial thrust per annuli
- Q = torque within annuli
- U_0 = flow rate incident on annuli inlet (front face of annuli)
- A = area of annuli inlet
- δC_T = local thrust coefficient from BEMT
- δC_P = local power coefficient from BEMT

The axial and tangential momentum source terms for the RANS domain are below. Note that the tangential term must be converted to a Cartesian coordinate system for use in the RANS equations.

$$f_x = \frac{T}{V} \tag{26}$$

$$f_\emptyset = \frac{Q}{rV} = \frac{Q}{r\Omega AL} \tag{27}$$

where:

- V = volume of annuli
- L = width of annuli
- r = radius out from centre of cylindrical region
- Ω = angular velocity

For the outermost annulus a tip loss factor is applied to account for the turbine blade not being infinite in length.

The RANS-BEMT approach allows for inclusion of wake swirl induced by the rotation of the turbine and rotor-induced drag without the need for a highly resolved mesh around each turbine blade. This allows for more accurate wake decay predictions as a function of the increased mixing introduced by the swirl. Recognising the link between wake growth and turbulence, this model also includes additional turbulent intensities to account for tip vortices and trailing edge effects. The turbulence downstream of a turbine, I_w, is a combination of the ambient turbulence, I_a; the shear induced turbulence, I_s, and the mechanical turbulence, I_m, caused by tip vortices and trailing edges.

$$I_w = I_a + I_m + I_s \tag{28}$$

The model accounts for I_a and I_s already. Turnock *et al.* [83] found that an additional turbulence intensity of 5% from I_m gave near-wake turbulent intensity profiles similar to those predicted by experiment

4.1.1 Benefits

- Well documented validation against experimental results.
- Can be run in parallel – limit on number of processors linked to mesh size but CFD codes designed for good parallel performance.
- Accounts for swirl effects from turbine rotation.
- Allows analysis of specific turbine blade design and yaw effects.
- Turbulence induced by tip vortices and trailing edges is included with additional injected turbulence without the need to refine the mesh.
- Contains turbulence closure and includes ambient turbulence in the channel.

4.1.2 Drawbacks

- Results are sensitive to mesh resolution.
- More computationally expensive than two-dimensional models – swept blade area meshed using 36 nodes radially and 76 nodes around the circumference [83].
- When using free-slip boundary conditions between span-wise neighbouring turbines, as is the case here, the model cannot consider wake mixing or device interaction between neighbouring rows of turbines. Modelling of more than a couple of rotors is problematic due to the high computational cost. Perhaps this model would assist in validation of a less computationally expensive model.

4.2 Low order blade induced turbulence model

A drawback of actuator disk approaches is that they inadequately model the turbulent mixing immediately behind the rotor. The reason for this is the lack of tip vortices when using a disk averaged approach. This less computationally expensive approach [90] includes correction functions behind the disk to account for tip vortex effects. These correction functions are applied to the turbulence model in the very near wake region. This is similar to the turbulent intensity injected into the wake by Turnock *et al.* [83].

Turbulence sources are based on expected values for the Reynolds shear stress. The standard k-ε model assumes isotropic turbulence. This does not hold true in the presence of tip vortices. Tip vortices create periodic adverse velocity profiles that appear as spikes in the long-term turbulence profile behind the disk as a vortex passes. However as you move downstream from the turbine this high level of anisotropy is mixed out and the effects of tip vortices can be thought of as isotropic.

4.2.1 Benefits

- Novel approach to accounting for blade-induced turbulence.
- Allows for tip vortex representation without the need to use actuator line or higher order model.

4.2.2 Drawbacks

- Little validation data or explanation available.

4.3 Turbulence timescale model - Modified ROMS

In the 3D Modified ROMS model [91] the Regional Ocean Modelling System (ROMS) has been modified to allow tidal current turbine representations. This model combines the low-resolution oceanographic modelling of large areas of open sea with detailed device-resolved actuator disk studies. The standard actuator disk assumptions for the coefficient of thrust, C_T, and power coefficient, C_P, are:

$$C_T = 4a(1-a) \tag{29}$$

$$C_P = 4a\ 1-a\ ^2 \tag{30}$$

where

- a is the axial induction factor – equivalent to the strength of velocity reduction across the disk.

The actuator disk approach limits the induction factor to $a \leq \frac{1}{2}$ or the flow behind the turbine reverses. The induction factor exceeds this limit in most real-life scenarios. The actuator disk approach removes the required amount of momentum from the flow to account for the power extraction of a turbine but does not account for device induced turbulence. When incorporated into a large-scale oceanographic model like ROMS, whose turbulence closure model sets a threshold of turbulence at a larger length and time scale than that of an actuator disk, the model must be modified to ensure it properly takes account of the turbulence in the wake of each tidal turbine.

This modification is carried out by adding source, sink, and turbulent cascade timescale terms to the turbulent kinetic energy transport equations. These account for turbine-induced turbulence, turbulent energy extraction by the disk, and reduced turbulence length spectra in the wake. These modifications are only carried out at the disk location.

By incorporating these additional turbulence timescales Roc *et al.* [91] improve on the standard actuator disk approach without the need to resolve the disk region further. In addition, when compared to the two previous large oceanographic modelling approaches listed in this report (where turbines were represented by additional drag terms alone – see chapters 4 and 5), the modified ROMS approach incorporates more device scale flow phenomena. This will lead to more accurate wake modelling and better power yield assessments of tidal arrays as a result.

4.3.1 Benefits

- Facilitates modelling of large-scale hydrodynamic impacts and device-scale effects within the same model.
- Models device interactions and wake mixings – crucial for array layout optimisation.
- Relatively low computational expense given the scale of simulations possible.
- Validated against the physical-scale models of Myers and Bahaj [92] as well as against data for multiple rotors [93].
- Model proven satisfactorily mesh independent with a minimum resolution of $\Delta x = 1D;\ \Delta y = \frac{1}{3}D$.

4.3.2 Drawbacks

- An odd number of lateral cells in the mesh yield better results.
- Results are sensitive to eddy viscosity – care must be taken in setting this with reference to the appropriate data.
- Horizontal shear in turbulent kinetic energy not accounted for in the ROMS model.

4.4 Turbulent kinetic energy and dissipation model – SNL-EFDC

Sandia National Laboratories environmental assessment modelling tool SNL-EFDC is a modified version of US Environmental Protection Agency's Environmental Fluid Dynamics Code ([94],[95],[96],[97]), coupled to both the US Army Corps of Engineers' water-quality code, CE-QUAL-ICM (Quality Integrated Compartment Model) ([98],[99]), and the sediment-dynamics code, SEDZLJ ([100],[101],[102],[103]). EFDC was developed to study river-, estuary-, coastal-, and ocean-scale systems and includes routines for the wetting and drying of regions and vegetative resistance. Depending on domain size and the number of grid cells, model runs can be completed in a matter of minutes for simple systems (<1,000 cells), and within a few hours for models of a complicated system (<10,000 cells) over a monthly tidal cycle. A new SNL-EFDC module considers energy removal from the flow system by Current Energy Converter (CEC) devices and the commensurate changes to the turbulent kinetic energy and its dissipation rate [104]. The CEC module provides a design tool capable of rapidly predicting power output and commensurate changes to the environment from a large number of field-scale CEC array configurations [104]; it is not intended to provide high-fidelity simulations of rotor hydrodynamics or detailed turbine wake structures. Once an array design has been chosen, more detailed simulations can be performed and layout optimized with SNL-EFDC.

The hydrodynamic portion of EFDC solves the hydrostatic, free surface, Reynolds Averaged Navier Stokes (RANS) equations with a Mellor-Yamada [77] turbulence closure, similar to the model of Blumberg and Mellor [105] except for the solution of the free surface, which is instead implemented with a preconditioned conjugate gradient solver. The standard Smagorinsky [106] k-ε turbulence model is implemented [107]. EFDC uses a curvilinear-orthogonal grid with a sigma, or stretched, vertical coordinate system ([96], [97]). Each sigma layer is assigned a constant (often equal) fraction of the flow depth throughout the model domain; where the absolute height of each layer changes with the topology of the model domain and water depth (i.e., at 10 m depth and 10 layers, each σ-layer would be 1 m thick, however, in the same model at 25 m depth, each layer would be 2.5 m thick). EFDC's time integration uses a second-order-accurate finite-difference scheme with an internal/external mode splitting procedure to separate the internal shear (or baroclinic mode calculated across each sigma layer) from the external free-surface gravity wave (or barotropic mode calculated on the depth average). EFDC has been extensively applied, validated and documented at numerous sites worldwide (e.g. [108], [109], [110], [111] to name a few). It has been applied to studies of estuaries, wetlands, lakes, rivers, and coastal environments ([112], [113], [114]). The model has been validated using analytical solutions, laboratory experiments, and real flow systems ([101], [104], [115]).

4.4.1 Benefits

- SNL-EFDC simulates device interactions and wake mixings and has been demonstrated to work very well in a power-optimization framework [116].
- Relatively low computational expense given the scale of simulations.
- Validated against the laboratory-scale flume experiments of Myers and Bahaj [117] and Neary et al. [118].
- The model can also simulate complicated sediment dynamics [101] and water quality ([119], [120]).

4.4.2 Drawbacks

- As a meso- to macro-scale model, SNL-EFDC is not designed to simulate the complicated turbulent wake structure immediately downstream (within three rotor diameters) of each device. CFD software and CFX or FLUENT should be used if this level of detail is required.
- The model is not parallelized (although commercial version of EFDC are available that run on multi-core machines).
- Only the k-ε turbulence closure scheme is available.
- Horizontal shear in turbulent kinetic energy not accounted for in the ROMS model.

GENERAL CONCLUSION AND RECOMMENDATION

The main purpose of Work Package 2 is to provide a tool that models the hydrodynamic interactions among the devices placed in an array and how it affects the resource, power performance, cost uncertainties and environmental impact. Detailed and reliable computational tools covering all those aspects for ocean energy array deployment are not available yet and it is far from clear what the dominant modelling technology will be in this sector. Therefore, specifying one method only from those detailed within this document may not be appropriate for the array deployment modelling tool within the DTOcean project.

For modelling arrays of wave energy converters, the PerAWaT project (Performance Assessment of Wave and Tidal Array Systems) will provide valuable lessons learnt for the work package to build upon. For example, the WaveFarmer planning tool developed within the PerAWaT project combines “spectral wave model”, “frequency domain BEM” and “time-domain BEM”. The computationally demanding time-domain BEM technique should be limited to uses of the tool where less than 10 units are deployed which could be suitable in situations such as for the westwave array which is a small wave energy device array to be deployed in West Clare Ireland [121], while the frequency-domain BEM could be an option for more than 10 deployed devices as it is the case for the West Lewis project to be deployed in West Lewis, Scotland and the Aegir Shetland Array project to be deployed in West Shetland, Scotland [121] for example. Wave propagation models provide important information related to the environmental impacts of the array deployment and would be very interesting to implement for the nearshore West Lewis project [121]. For some of the scenarios it could also be relevant to combine frequency-domain BEM with wave propagation model to benefit from the two types of model as proposed by Babarit *et al.* [122]. Further analysis is required before deciding if incorporation of the frequency-domain or time-domain BEM directly into the DTOcean tool is too computationally demanding. A solution to this would be to build a data base from a pre-compiled range of chosen parameters and use that data base in the DTOcean tool.

Concerning the modelling of arrays of tidal energy converters, models such as the "SNL-EFDC" model, the "Modified ROMS" model or the "low order blade induced turbulence" model stand out as the most relevant approaches for tidal turbine array simulation However, they are all too computationally expensive as well as unnecessarily accurate, in respect to the requirements of a generic decision making tool and the scope of work of DTOcean. Accordingly, parametric methods should prevail. At the present stage of the project, the model design recommendation would be to follow a similar approach to that of the "TidalFarmer" by combining three parametric sub-models respectively accounting for "blockage effects", "near wake induced turbulences" and "far wake mixing". Another option would be to use the "Semi-empirical wake" model and/or "Parametric farm's blockage and efficiency" model. Nonetheless, in every possible scenario, an extensive validation database will be required in order to produce valid empirical relationships, the quintessence of any parametric method. This data shall describe the performance and wake hydrodynamic characteristics of a standalone device subject to a wide range of inflows

representative of the tidal regimes encountered at the site under consideration and also the modified inflows within the array. This database shall be based on existing studies from DTOcean partners as well as, if necessary, CFD simulations.

REFERENCES

[1] K. Budal (1977). Theory of absorption of wave power by a system of interacting bodies. Journal of Ship Research 21, 248-253.

[2] D.V. Evans (1979). Some theoretical aspects of three-dimensional wave-energy absorbers. Proceedings of the 1st Symposium on Wave Energy Utilisation, Gothenburg, Sweden.

[3] J. Falnes (1980). Radiation impedance matrix and optimum power absorption for interacting oscillators in surface waves. Applied Ocean Research 2, 75-80.

[4] P. McIver (1994). Some hydrodynamic aspects of arrays of wave-energy devices. Applied Ocean Research 16, 61-69.

[5] M.J. Simon (1982). Multiples scattering in arrays of axisymmetric wave-energy devices – a matrix method using a plane wave approximation. Journal of Fluid Mechanics 120, 1-25.

[6] J. Falnes, K. Budal (1982). Wave-power absorption by parallel rows of interacting oscillating bodies. Applied Ocean Research 4, 194-207.

[7] P. McIver (1984). Wave forces on arrays of floating bodies. Journal of Engineering Mathematics 18, 273-285.

[8] S.A. Mavrakos (1991). Hydrodynamic coefficients for groups of interacting vertical axisymmetric bodies. Ocean Engineering 18, 485-515

[9] S.A. Mavrakos, P. Koumoutsakos (1987). Hydrodynamic interactions among vertical axisymmetric bodies restrained in waves. Applied Ocean Research 9, 128-140.

[10] S.A. Mavrakos, A. Kalofonos (1997). Power absorption by arrays of interacting vertical axisymmetric wave-energy devices. Journal of Offshore Mechanics and Artic Engineering 119, 244-249.

[11] X. Garnaud, C. C. Mei (2010). Bragg scattering and wave-power extraction by an array of small buoys. Proceedings of the Royal Society A 466, 79-106.

[12] H. Kagemoto, D.K.P. Yue (1986). Interactions among multiple three-dimensional bodies in water waves: an exact algebraic method. Journal of Fluid Mechanics 166, 189-209.

[13] B.F.M. Child, V. Venugopal (2010). Optimal configurations of wave energy device arrays. Ocean Engineering 37, 1402-1417.

[14] P. Justino, A. Clement (2003). Hydrodynamic performance for small arrays of submerged spheres. Proceedings of the 5th European Wave Energy Conference, Cork, Ireland.

[15] P. Ricci, J. Saulnier, A. Falcao (2007). Point-absorbers arrays : a configuration study off the Portugese west-coast. Proceedings of the 7th European Wave and Tidal Energy Conference, Porto, Portugal.

[16] G. De Backer, M. Vantorre, C. Beels, J. De Rouck, P. Frigaard (2009). Performance of closely spaced point absorbers with constrained floater motion. Proceedings of the 8th European Wave and Tidal Energy Conference, Uppsala, Sweden.

[17] P.C. Vicente, A.F. de O. Falcão, L.M.C. Gato, P.A.P. Justino (2009). Dynamics of arrays of floating point-absorber wave energy converters with inter-body and bottom slack-mooring connections. Applied Ocean Research 31, 267-281.

[18] A. Babarit (2010). Impact of long separating distances on the energy production of two interacting wave energy converters. Ocean Eng. 37. 718-729.

[19] B. Borgarino, A. Babarit, P. Ferrant (2012). Impact of wave interactions effects on energy absorption in large arrays of wave energy converters. Ocean Engineering 41, 79-88.

[20] A. Babarit (2013). On the park effect in arrays of oscillating wave energy converters. Renewable Energy 58, 68-78.

[21] R. Taghipour, T. Moan (2008). Efficient Frequency-Domain Analysis of Dynamic Response for the Multi-Body Wave Energy Converter in Multi-Directional Waves. Proceedings of the 18th International Offshore and Polar Engineering Conference, Vancouver, Canada.

[22] WAMIT (2013). WAMIT® USER MANUAL Version 7.0 [Online]. Available: www.wamit.com [Accessed 13 March 2014].

[23] ANSYS Aqwa (2012). AQWA User Manual. [Online]. Available: http://www.ansys.com/Products/Other+Products/ANSYS+AQWA

[24] G. Delhommeau (1993). Seakeeping codes Aquadyn and Aquaplus. In 19th WEGMENT School, Numerical Simulation of Hydrodynamics: Ship and Offshore Structures.

[25] Ben Child (2013). Performance Assessment of Wave and Tidal Array systems (PerAWaT), Wave [Online]. Available: http://www.gl-garradhassan.com/assets/downloads/WaveFarmer.pdf [Accessed 13 March 2014].

[26] Nemoh (2014). http://lheea.ec-nantes.fr/doku.php/emo/nemoh/start [Accessed 13 March 2014].

[27] M. Folley, A. Babarit, B. Child, D. Forehand, L. O'Boyle, K. Silverthorne, J. Spinneken, V. Stratigaki, P. Troch (2012). A review of numerical modelling of wave energy converter arrays. Proceedings of the ASME 2012 31st International Conference on Ocean, Offshore and Arctic Engineering, Rio de Janeiro, Brazil.

[28] R. Taghipour, T. Perez, and T. Moan (2008). Hybrid frequency-time domain models for dynamic response analysis of marine structures. Ocean Engineering 35, 685-705.

[29] TiMIT (1999). TiMIT A panel-method program for transient wave-body interactions [Online]. Available: http://www.wamit.com/Publications/TiMITmanual.pdf [Accessed 13 March 2014].

[30] A. Babarit, A.H. Clément (2006). Optimal latching control of a wave energy device in regular and irregular waves. Applied Ocean Research 28, 77-91.

[31] A.P. McCabe, G.A. Aggidis, T.J. Stallard (2006). A time-varying parameter model of a body oscillating in pitch. Applied Ocean Research 28, 359-370.

[32] M. Kashiwagi (2000). Non-linear simulations of wave-induced motions of a floating body by means of the mixed Eulerian-Lagrangian Method. Proceedings of the institution of mechanical engineers, Part C: Journal of Mechanical Engineering 214, 841-855.

[33] C. Hague, C. Swan (2009). A Multiple flux boundary element method applied to the description of surface water waves. Journal of Computational Physics 228, 5111-5128.

[34] E. Guerber, M. Benoit, S. T. Grilli, C. Buvat, Modeling of Fully Nonlinear Wave Interactions with Moving Submerged Structures. Proceedings of the 20th International Offshore and Polar Engineering Conference, Beijing, China.

[35] P.A. Madsen, O.R. Sorensen (1992). A new form of the Boussinesq equations with improved linear dispersion characteristics Part 2: A slowly-varying bathymetry. Coastal Engineering 18, 183-204.

[36] M. Ricchiuto, A. G. Filippini (2014). Upwind residual discretization of enhanced Boussinesq equations for wave propagation over complex bathymetries. Journal of Computational Physics, *Article in press*.

[37] MIKE 21 BW (2011). Boussinesq waves module user guide. Danish Hydraulic Institute.

[38] V. Venugopal, G.H. Smith (2007). Wave Climate investigation for an array of wave power devices. Proceedings of the 7th European wave and tidal energy conference, Porto, Portugal.

[39] J.H. Nørgaard, T.L. Andersen (2012). Investigation of Wave Transmission from a floating Wave Dragon Wave Energy Converter. Proceedings of the 22nd International Offshore and Polar Engineering Conference, Rhodes, Greece.

[40] P. Troch (1998). Mildwave – a numerical model for propagation and transformation of linear water waves. Department of civil engineering, Ghent University, Ghent.

[41] A.C. Radder and M.W. Dingemans (1985). Canonical equations for almost periodic, weakly nonlinear gravity waves. Wave Motion 7, 473-485.

[42] J.T. Kirby and R.A. Dalrymple (1994). REF/DIF 1 Version 2.5 Documentation and User's Manual. Center for Applied Coastal Research, Department of Civil Engineering, University of Delaware, Newark.

[43] M. González, R. Medina, J. Gonzalez-Ondina, A. Osorio, F.J. Méndez, and E. García (2007). An integratedcoastal modelling system for analysing beach processes and beach restoration projects, SMC. Computers & Geosciences 33, 916-931.

[44] L.H. Holthuijsen, A. Herman, N. Booij (2003). Phase-decoupled refraction-diffraction for spectral wave models. Coastal Engineering 49, 291-305.

[45] N. Booij, R.C. Ris, L.H. Holthuijsen (1999). A Third-generation wave model for coastal regions 1. Model description and validation. Journal of Geophysical research 104, 7649-7666.

[46] M. Benoit, F. Marcos, F. Becq (1996). Development of a third-generation shallow-water wave model with unstructured spatial meshing. Proceedings of the 25th International conference on coastal Engineering, Orlando, USA.

[47] D.L. Millar, H.C.M. Smith, D.E. Reeve (2007). Modelling analysis of the sensitivity of shoreline change to a wave farm. Ocean Engineering 34, 884-901.

[48] H.C.M. Smith, C. Pearce, D.L. Millar (2012). Further analysis of change in nearshore wave climate due to an offshore wave farm: an enhanced case study for the wave hub site. Renewable energy 40, 51-64.

[49] K. Ruehl, A. Porter, A. Posner and J. Roberts (2013) Sandia National Laboratories: Development of SNL-SWAN, a Validated Wave Energy Converter Array Modeling Tool

[50] SWAN (2013). User Manual SWAN Cycle III version 40.91ABC. Delft University of Technology.

[51] K. Silverthorne, M. Folley (2011). A New numerical representation of wave energy converters in a spectral wave model. Proceedings of the 9th European Wave and Tidal Energy Conference, Southampton, UK.

[52] M. Folley, T. Whittaker (2010). Spectral Modelling of Wave energy converters. Coastal Engineering 57, 892-897.

[53] TOMAWAC (2011). Software for sea state modelling on unstructured grids over oceans and coastal seas. EDF R&D.

[54] D. Thévenin and G. Janiga (2008). Optimization and Computational Fluid Dynamics, Berlin: Springer.

[55] R. Vennell (2011). Tuning tidal turbines in-concert to maximise farm efficiency. Journal of Fluid Mechanics 671, 587-604.

[56] R. Vennell (2010). Tuning Turbines in a Tidal Channel. Journal of Fluid Mechanics 663, 253-267.

[57] C. Garrett and P. Cummins (2005). The power potential of tidal currents in channels. Proc. of the Royal Society A-Mathematical Physical and Engineering Sciences 461(2060), 2563-2572.

[58] C. Garrett and P. Cummins (2007). The efficiency of a turbine in a tidal channel. Journal of Fluid Mechanics 588, 243-251.

[59] M. Palm, R. Huijsmans and M. Pourquie (2011). The applicability of semi-empirical wake models for tidal farms. Proceedings of the 9th European Wave and Tidal Energy Conference, Southampton, UK.

[60] T. Nishino and R. H. J. Wilden (2012). The efficiency of an array of tidal turbines partially blocking a wide channel. Journal of Fluid Mechanics 708, 596-606.

[61] S. G. Parkinson, T. Stallard, M. Thomson, A. Wickham and R. Willden (2012). Comparison of scale model wake data with an energy yield analysis tool for tidal turbine farms. Proceedings of the 4th International Conference on Ocean Energy (ICOE), Dublin, Ireland.

[62] J. F. Ainslie (1988). Calculating the flowfield in the wake of wind turbines. Journal of Wind Engineering and Industrial Aerodynamics 27, 213-224.

[63] R. L. Burden and J. D. Faires (2005). Numerical Analysis, Belmont: Thomson Brooks & Cole.

[64] A. Duckworth and R. J. Barthelmie (2008). Investigation and validation of wind turbine wake models. Journal of Wind Engineering 32, 459-475.

[65] R. Ahmadian and R. Falconer (2012). Assessment of array shape of tidal stream turbines on hydro-environmental impacts and power output. Renewable Energy 44, 318-327.

[66] S. Nash (2007). A nested version of the combined hydrodynamic and water quality model, DIVAST. Proceedings of the 11th International Conference on Civil, Structural and Environmental Engineering Computing, St. Julians, Malta.

[67] R. Falconer and G. Li (1992). Modeling tidal flows in an Islands Wake using a 2-equation Turbulence model. P I Civil Eng-Water 96, 43-53.

[68] D. Fallon, M. Hartnett, A. Olbert and S. Nash (2014). The effects of array configuration on the hydro-environmental impacts of tidal turbines. Renewable Energy 64, 10-25.

[69] R. Ahmadian, R. Falconer and B. Lin (2010). Hydro-environmental modelling of proposed Servern barrage. UK, P Civil Eng Energy 163, 107-117.

[70] T. Divett, R. Vennell and C. Stevens (2011). Optimisation of multiple turbine arrays in a channel with tidally reversing flow by numerical modelling with adaptive mesh. Proceedings of the 9th European Wave and Tidal Energy Conference, Southampton, UK.

[71] S. Popinet and G. Rickard (2007). A tree-based solver for adaptive ocean modelling. Ocean Modelling 16, no. 3-4, 224-249.

[72] R. Flather (1976). A tidal model of the northwest European continental shelf. Memoires de la Societe Royale de Sciences de Liege 6, 141-164.

[73] S. Draper, G. Houlsby, M. Oldfied and A. Borthwick (2010). Modelling tidal energy extraction in a depth-averaged coastal domain. Renewable Power Generation 4, no. 6, 545-554.

[74] L. Blunden and A. Bahaj (2008). Flow through large arrays of tidal energy converters: is there an anolgy with depth limited flow through vegetation?. World Renewable Energy Congress (WRECX).

[75] S. Neill, J. Jordan and S. Couch (2012). Impact of tidal energy converter (TEC) arrays on the dynamics of headland sand banks. Renewable Energy 37(1), 387-397.

[76] J. Holt (2008). POLCOMS User Guide. Coastal Observatory, Liverpool, UK.

[77] G. Mellor and T. Yamada (1982). Development of a turbulence closure model for geophysical fluid problems. Reviews of Geophysics and Space Physics 20, 851-875.

[78] S. Bourban, M. Liddiard, N. Durand, S. Cheeseman and A. Baldock (2013). High resolution modelling of tidal resources, extraction and interactions around the UK. Proceedings of the 1st Marine Energy Technology Symposium, 1-8, Washington D.C., USA.

[79] H. Wallingford (2010). TELEMAC modelling system: User Manual, V6.0. EDF, Chatou, France.

[80] WHCMSC, "THREDDS Data Server - dataset: tpxo/tpxo7.2_uv.nc," WHCMSC Sediment Transport Group, 30 12 2010. [Online]. Available: http://geoport.whoi.edu/thredds/catalog/usgs/vault0/models/tides/tpxo/catalog.html?dataset=usgs/vault0/models/tides/tpxo/tpxo7.2_uv.nc. [Accessed 12 March 2014].

[81] A. Perez-Ortiz, J. Pescatore and I. Bryden (2013). A systematic approach to undertake tiday energy resource assessment with Telemac-2D. Proceedings of the 10th European Wave and Tidal Energy Conference, Aalborg, Denmark.

[82] C. Moulinec, C. Denis, C.-T. Pham, D. Rougé, J.-M. Hervouet, E. Razafindrakoto, R. Barber, D. Emerson and X.-J. Gu (2011). TELEMAC: An efficient hydrodynamics suite for massively parallel architectures. Computers & Fluids 51, no. 1, 30-34.

[83] S. Turnock, A. Phillips, J. Banks and R. Nicolls-Lee (2011). Modelling tidal current turbine wakes using a coupled RANS-BEMT appraoch as a tool for analysing power capture of arrays of turbines. Ocean Engineering 38 (11-12), 1300-1307.

[84] R. Malki, I. Masters, A. Williams and T. Croft (2014). Planning tidal stream turbine array layouts using a couples blade element momentum - computational fluid dynamics model. Renwable Energy, 46-54.

[85] L. Ju Hyun, P. Sunho, D. H.K., S. H.R. and K. Moon-Chan (2012). Computational methods for performance analysis of horizontal axis tidal stream turbines. Applied Energy 98, 512-523.

[86] M. Barnsley and J. Wellicome (1993). Dynamic models of wind turbines - Final report on contract JOUR 0110 for the Comission of the European Communities Directorate. General XII Science, Research and Development.

[87] T. Purcell (2011). Blade Element Momentum Theory applied to horizontal axis wind turbines - PhD Thesis. The Pennsylvania State University - Department fo Aerospace Engineering, Indianapolis.

[88] M. Drela (1989). XFOL: An Analysis and Design System for Low Reynolds Number Airfoils. Proceedings of the Conference on low Reynolds number airfoil aerodynamics, University of Notre Dame, USA.

[89] S. Turnock (2006). Predictions of Hydrodynamic Performance of Horizontal Axis Tidal Turbines. Report 1878. Wolfson Unit for Marine Technology and Industrial Aerodynamics.

[90] T. Nishino and R. Willden (2012). Low-order modelling of blade-induced turbulence for RANS Actuator Disk Computations of wind and tidal turbines. EUROMECH Colloquium 528: Wind Energy and the Impace of Turbulence on Conversion Process, Oldenburg, Germany.

[91] T. Roc, D. Conley and D. Greaves (2013). Methodology for tidal turbine representation in ocean circulation model. Renewable Energy 51, 448-464.

[92] L. Myers and A. Bahaj (2010). Experimental analysis of the floe field around horizontal axis tidal turbines by use of scale mesh disk rotor simulators. Ocean Engineering 37, 218-227.

[93] T. Roc, D. Greaves, K. Thyng and D. Conley (2014), Tidal turbine represenation in an ocean circulation model: Towards realistic applications. In press in Ocean Engineering.

[94] J. Hamrick (1992). Three-Dimensional Environmental Fluid Dynmaics Computer Code: Theoretical and Computational Apsects. The College of William and Mary, p. 63.

[95] J. Hamrick (1996). User's Manual for the Environmental Fluid Dynamics Computer Code, Gloucester Point, Virginia: Virginia Institute of Marine Sciences.

[96] J. Hamrick (2007). The Environmental Fluid Dynamics Code: User Manual, Fairfax, VA: US EPA.

[97] J. Hamrick (2007). The Environmental Fluid Dynamics Code: Theory and Computation, Fairfax, VA: US EPA.

[98] C. Cerco and T. Cole (1995). User's Guide to the CE-QUAL-ICM Three-Dimensional Eutrophication Model, Release Version 1.0, Washington, DC, U.S Army Corps of Engineers, p. 316.

[99] K. Park, A. Kuo, J. Shen and J. Hamrick (1995). A three-dimensional hydrodynamic-eutrophication model (HEM-3D): Description of water quality and sediment process submodels, Gloucester Point, Virginia: Virginia Institute of Marine Science.

[100] S. James, M. Grace, M. Ahlmann, C. Jones and J. Roberts (2008). Recent advances in sediment transport modeling. Proceedings of the 2008 World Environmental and Water Resources Congress, American Society of Civil Engineers, Honalulu, Hawaii.

[101] S. James, C. Jones, M. Grace and J. Roberts (2010). Advances in sediment transport modelling. Journal of Hydraulic Research 48, 754-763.

[102] C. Jones and W. Lick (2001). Sediment erosion rates: Their measurement and use in modeling. Proceedings of the Texas A&M Dredging Seminar, Sanford, L.P., Ed. ASCE, p1-15, College Station, Texas, USA.

[103] W. Lick, Z. Chroneer, C. Jones and R. Jepsen (1998). A predictive model of sediment transport. Estaury and Coastal Modeling, Spaulding, M.L, Blumberg, A.F., Eds. Alexandria, VA.

[104] S. James, E. Seetho, C. Jones and J. Roberts (2010). Simulating environmental changes due to marine hydrokinetic energy installations. OCEANS 2010, Spindel, B.; Brockett, T. pp 1-10, Eds. Seattle, WA, USA.

[105] A. Blumberg and G. Mellor (1987). A description of a three-dimensional coastal ocean circulation model. Proceedings of the Three Dimensional Coastal Ocean Models, Heaps, N.S., Ed. American Geophysical Union, Vol. 4, pp 1-16, Washington, DC, USA.

[106] J. Smagorinsky (1963). General circulation experiments with primitive equations 1: The basic experiment. Monthly Weather Review 91, 99-164.

[107] Y. Chen and S. Kim (1987). Computation of Turbulent Flow Using an Extended Turbulence Closure Model. NASA, p.22.

[108] S. Peng, G. Fu, X. Zhao and B. Moore (2011). Integration of Environmental Fluid Dynamics Code (EFDC) Model with Geographical Information System (GIS) Platform and Its Applications. Journal of Environmental Informatics 17, 75-82.

[109] B. Tuckey, M. Gibbs, B. Knight and P. Gillespie (2006). Tidal circulation in Tasman and Golden Bays: implications for river plume behaviour. New Zealand Journal of Marine and Freshwater Research 40, 305-324.

[110] Z.-G. Ji (2008). Hydrodynamics and Water Quality: Modeling Rivers, Lakes, and Estuaries. Hoboken, NJ, John Wiley and Sons, p. 676.

[111] Z. Ji, M. Morton and J. Hamrick (2001). Wetting and Drying Simulation of Estuarine Processes. Estuarine, Coastal and Shelf Science 53, 683-700.

[112] M. Moustafa and J. Hamrick (2000). Calibration of the Wetland Hydrodynamic Model to the Everglades Nutrient Removal Project. Water Quality and Ecosystems Modeling 1, 141-167.

[113] K. Jin, Z. Ji and J. Hamrick (2002). Modeling winter circulation in Lake Okeechobee, Florida. Journal of Waterway, Port, Coastal, and Ocean Engineering, p. 128.

[114] M. Xia, P. Craig, C. Wallen, A. Stoddard, J. Mandrup-Poulsen, M. Peng, B. Schaeffer and Z. Liu (2011). Numerical Simulation of Salinity and Dissolved Oxygen at Perdido Bay and Adjacent Coastal Ocean. Journal of Coastal Research 27, pp. 73-86.

[115] S. James, J. Barco, E. Johnson, J. Roberts and S. Lefantzi (2011). Verifying marine-hydro-kinetic energy generation simulations using SNL-EFDC. Oceans 2011, Kenoi, B.; Taylor, B., Eds. pp 1-9, Kona, HI.

[116] K. Nelson, C. Jones, J. Roberts and S. James (2014). A framework for optimizing the placement of current energy converters. Proceedings of the 7th Annual Global Marine Renewable Energy Conference, Seattle, USA.

[117] L. Myers and A. Bahaj (2012). An experimental investigation simulating flow effects in first generation marine current energy converter arrays. Renewable Energy 37, 28-36.

[118] V. Neary, B. Gunawan, C. Hill and L. Chamorro (2012). Wake flow recovery downstream of a 1:10 scale axial flow hydrokinetic turbine measured with pulse-coherent acoustic Doppler profiler (PC-ADP). Oak Ridge National Laboratory, Oak Ridge, TN.

[119] S. James and V. Boriah (2010). Modeling algae growth in an open-channel raceway. Journal of Computational Biology 17, 895-906.

[120] S. James, V. Janardhanam and D. Hanson (2013). Simulating pH effects in an algal-growth hydrodynamics model. Journal of Phycology 49, 608-615.

[121] DTOcean Project Deliverable 1.1 (2014). Detailed Deployment Scenarios for wave and tidal energy converters.

[122] A. Babarit, M. Folley, F. Charrayre, C. Peyrard, M. Benoit (2013). On the modelling of WECs in wave models using far field coefficients. Proceedings of the 10th European Wave and Tidal Energy Conference, Aalborg, Denmark.